A unified formulation for static behavior
of nonlocal curved beams

Ekrem Tufekci[*], Serhan A. Aya[a] and Olcay Oldac[b]

Istanbul Technical University, Faculty of Mechanical Engineering, Gumussuyu 34437, Istanbul, Turkey

Abstract.   Nanobeams are widely used as a structural element for nanodevices and nanomachines. The development of nano-sized machines depends on proper understanding of mechanical behavior of these nano-sized beam elements. Small length scales such as lattice spacing between atoms, surface properties, grain size etc. are need to be considered when applying any classical continuum model. In this study, Eringen's nonlocal elasticity theory is incorporated into classical beam model considering the effects of axial extension and the shear deformation to capture unique static behavior of the nanobeams under continuum mechanics theory. The governing differential equations are obtained for curved beams and solved exactly by using the initial value method. Circular uniform beam with concentrated loads are considered. The displacements, slopes and the stress resultants are obtained analytically. A detailed parametric study is conducted to examine the effect of the nonlocal parameter, mechanical loadings, opening angle, boundary conditions, and slenderness ratio on the static behavior of the nanobeam.

1. Introduction

Nano-sized beam structures have great potential applications in many different fields such as nanoscale actuation, sensing, and detection due to their remarkable mechanical, electronic and chemical properties. High stiffness and strength, low density and good conductivity have made nanobeams the foundation building element for nano electro-mechanical devices, ultrasensitive sensors, semiconductor nanowires, atomic force microscopy etc. (Kong *et al.* 2000, Li and Chou 2003, Craighead 2000, Roukes 2001, Ekinci 2005). As a particular example, with small size and large surface, carbon nanotubes stand out with their persistency in harsh chemical environment (Zhao *et al.* 2002) and can respond to the external mechanical deformation rapidly with high sensitivity. Scale of these materials makes experimental studies very challenging. Though, a common result from the experimental studies in some metals and polymers is the size dependence of mechanical properties and material deformation behavior in micro and nano-scale. The Young's

∗Corresponding author, Professor, E-mail: tufekcie@itu.edu.tr
[a]Ph.D. Student, E-mail: ayas@itu.edu.tr
[b]Ph.D. Student, E-mail: olcay.oldac@tr.kspg.com

modulus was found to be extremely high in several experimental studies (Treacy *et al.* 1996, McFarland and Colton 2005). Since the properties of nano materials are distinctly different from those of the bulk material, they offer great potential applications and superior performance. In view of this, it is of great significance to gain a full understanding of the static properties of nanobeams.

In pursuit of understanding the mechanical behavior of nano-sized materials, molecular dynamics (MD) simulations enable comparable investigations of dynamics of nano-materials to experiments, and further bring out detailed information on interatomic interactions of nano-materials and molecular complexes, which is essential for developing advanced experiments (Arash *et al.* 2011). Besides the experiments and MD simulations, continuum mechanics approach has also been considered for modeling nanobeams. Continuum models presented in literature are generally based on classical (or local), and nonlocal continuum theories. In the classical continuum models, stress state at a given point is determined by the strain state at the same point. They are less computationally expensive, however, inherent restriction of classical continuum models, i.e., elimination of structural discontinuity at the atomic scale, reliability of the results of classical models for the mechanical behavior of micro and nano structures is questioned. In order to resolve the limitation, several useful theories and applications of the nonlocal continuum mechanics, which allows the small scale effects to be included in analysis of nano materials have been implemented in the studies. Couple stress theory, is a size-dependent continuum mechanics model for the analysis of nanostructures which uses virtual work and kinematical assumptions to explain the skew-symmetric nature of the couple-stress tensor and shows that mean curvature is in fact the correct energy conjugate measure of deformation (Hadjesfandiari and Dargush 2011). This theory is applied for the static bending and free vibration problems of a simply supported curved beam (Liu and Reddy 2011) and it is concluded that the predicted trends confirm the size effect at the micron scale observed in the experiments. Berrabah *et al.* (2013) proposed a unified nonlocal shear deformation theory to study the bending, buckling and free vibration of nanobeams. Both small scale effect and transverse shear deformation effects of nanobeams were considered in the model and Hamilton's principle was used for obtaining equations of motion and analytical solutions were presented for the deflection, buckling load, and natural frequency of a simply supported nanobeam. Recently, another size-dependent continuum approach, strain gradient theory became very popular and different microbeam and microplate models are developed based on this theory. Akgoz and Civalek (2013) investigated the buckling problem of linearly tapered micro-columns by using a modified strain gradient elasticity theory. Bernoulli-Euler beam theory was used to model the micro column and Rayleigh-Ritz method was utilized to obtain the solution. Li (2013) studied the transverse vibrations of axially traveling nanobeams including strain gradient and thermal effects and used the variational principle to obtain the differential equation of motion. Effects of nanoscale parameter, temperature change, shape parameter and axial traction on the natural frequencies were discussed through the examples.

Among the size-dependent continuum mechanics models for the analysis of nanostructures, the most popular approach is Eringen's integral theory or nonlocal elasticity theory (Eringen, 1983). This theory states that the stress at a given reference point of a body is a function of the strain field at every point in the body; hence, the theory takes the long range forces between atoms and the scale effect into account in the formulation. Application of nonlocal elasticity for the formulation of nonlocal version of the Euler-Bernoulli beam model is initially proposed by Peddieson *et al.* (2003). Since then, the nonlocal theory, including nano-beam, plate and shell models were successfully developed using nonlocal continuum mechanics and many researchers reported on

bending, vibration, buckling and wave propagation of nonlocal nanostructures (Wang 2005, Wang and Shindo 2006, Polizzotto *et al.* 2006). Reddy (2007) improved existing classical Euler-Bernoulli, Timoshenko, Levinson and Reddy beam theories by implementing nonlocal differential constitutive equations. Pradhan and Sarkar (2009) studied the bending, buckling and vibration of tapered functionally graded beams by using Eringen's non-local elasticity theory. Both Euler-Bernoulli and Timoshenko beam theories were considered and Rayleigh-Ritz method was used for the solution. Paola (2013) investigated the dynamics of a nonlocal Timoshenko beam by modeling nonlocal effects as long-range volume forces and moments mutually exerted by nonadjacent beam segments. In this manner, various sources of nonlocal effects were addressed and pertinent applications were discussed. Behera and Chakraverty (2014) studied the free vibration of nonhomogeneous nanobeams based on nonlocal theory using boundary characteristic orthogonal polynomial functions in the Rayleigh–Ritz method. A finite element method was presented for a nonlocal Timoshenko beam model by Alotta *et al.* (2014). For most common attenuation functions of nonlocal effects, exact closed-form solutions found for every element of the nonlocal stiffness matrix. Numerical applications were presented for a variety of nonlocal parameters, including a comparison with experimental data. Zemri *et al.* (2015) presented a nonlocal shear deformation beam theory for bending, buckling, and vibration of functionally graded (FG) nanobeams by using Eringen's nonlocal constitutive relations. Higher-order variation of transverse shear strain through the depth of the nanobeam was considered, therefore, shear correction factor was not required. Zhang *et al.* (2015) proposed a microstructured beam-grid model for the vibration of initially stressed rectangular plates with simply supported edges. Based on the model, exact small length-scale coefficients were determined for the vibration problem of the initially stressed plate. Taghizadeh *et al.* (2015) presented a 2-D finite element formulation by using the nonlocal integral elasticity. The bending problem of a nanobeam was solved based on classical beam theory and also 3-D elasticity theory using nonlocal finite elements. Comparison of the results with the relevant literature demonstrate that the scale effect on mechanical responses of nanostructures can be predicted successfully by the nonlocal elasticity theory. In another important study, a new analytical approach considering the effective nonlocal shear stress field is proposed by Li (2014). In the model, nano-structural stiffness of cylindrical nanostructures is enhanced with stronger nonlocal effects. On the contrary, some studies show that increasing nonlocal effect increases the deformation. Therefore, two kinds of nonlocal models are present: The nonlocal strengthening model and the nonlocal softening model. The difference is caused by different surface effects such as the long range attractive and repulsive interactions between atoms on the surface. Both models are proved to be valid by the work of Li *et al.* (2015a, b).

Most of these studies focused on straight beam formulation, however, it is known that these structures might not be perfectly straight (Joshi *et al.* 2010). As an example, carbon nanotubes are long and bent, the bending being observed in isolated carbon nanotubes between electrodes or composite systems made from carbon nanotubes (Guo *et al.* 2000). The curvature may be originated from buckling of axially loaded straight nanotubes or it is a result of fabrication and waviness affects the material stiffness. Although carbon nanotubes are usually not straight and have some waviness along its length, few investigations are known to be concerned with the vibration of these nanostructures. Fisher *et al.* (2003) and Bradshaw *et al.* (2003) used micromechanical methods for modelling and combined with finite element results. The study revealed the importance of the curvature of a nanotube, because compared to the straight nanotubes, the effective reinforcement is significantly reduced. As another example, classical Euler-Bernoulli theory is applied by Mayoof and his co-worker Hawwa (2009) for the

investigation of nonlinear vibration of a single-walled carbon nanotube with waviness along its axis. The carbon nanotube was modeled as a harmonically excited beam under a transverse force. Dynamic response was investigated in the context of the bifurcation and chaos theory.

In the study, in-plane static behavior of a planar curved nanobeam is investigated. Exact analytical solution of in-plane static problems of a circular nanobeam with uniform cross-section is presented. It is known that the size elimination of the nano scale effect may cause a significant deviation in the results. This study aims to overcome the problem by using Eringen's nonlocal theory. Initially, the governing differential equations of static behavior of a curved nanobeam are given by using the nonlocal constitutive equations of Eringen. The expressions for components of Laplacian of the symmetrical second order tensor in cylindrical coordinates given by Povstenko (1995) are implemented in Eringen's nonlocal equations in order to obtain the governing equations of a curved beam in Frenet frame. Based on the initial value method, the exact solution of the differential equations is obtained. The displacements, rotation angle about the binormal axis and the stress resultants are obtained analytically. The axial extension and shear deformation effects are considered in the analysis. A parametric study is also performed to point out the effects of the geometric parameters such as slenderness ratio, opening angle, loading and boundary conditions. To the authors' best knowledge, almost all of the studies on the nonlocal beam theory has been discussed in the context of straight nanobeams. There is very limited number of papers on the curved nanobeams and most of them neglect the effects of axial extension and shear deformation. They use numerical and approximate solution methods and consider only the nonlocal effect of bending moment. However, the results confirm a particular conclusion that bending deformation of the nano-cantilever beam subjected to a concentrated force reveals no nonlocal effect (Li *et al.* 2015b). The present work will be helpful in the analysis and design of circular nanobeams with various combinations of loadings, boundary conditions and material properties.

2. Analysis

Integral and gradient type nonlocal theories which include the characteristic length are used to solve the problems of micro and nano beams. The characteristic length depends on lattice parameter, granular size or molecular diameters. When the size of the beam is much larger than the characteristic length, the results of the nonlocal theories converge to those of the local theory. Nonlocal elasticity theories were proposed by several authors (Eringen 1983, Peddieson *et al.* 2003). According to Eringen's nonlocal model, the stress values at a generic point are related to a weighted integral of strains over a certain domain. In isotropic media, it is assumed that a unique kernel weights all entries of stiffness tensor equally (Eringen 1983), and the equation is given as

$$\sigma_{ij}^{nl}(\boldsymbol{x}) = \int_{\Omega} \alpha(\boldsymbol{x}, \boldsymbol{x}') \, \sigma_{ij}^{l}(\boldsymbol{x}') \, d\Omega \tag{1}$$

where σ_{ij}^{nl} and σ_{ij}^{l} are nonlocal and local stress tensors, respectively, $\boldsymbol{x}$ and $\boldsymbol{x}'$ are position vectors for two material points in domain Ω and α is a scalar kernel function. The integral constitutive equations of nonlocal elasticity can be simplified to an equivalent partial differential equation by making certain assumptions (Eringen 1983)

$$(1 - \gamma^2 \nabla^2)\boldsymbol{\sigma}^{nl} = \boldsymbol{\sigma}^{l} \tag{2}$$

where ∇^2 is the Laplacian operator, $\boldsymbol{\sigma}^{nl}$ and $\boldsymbol{\sigma}^{l}$ are the nonlocal and local stress tensors,

respectively, and $\gamma = e_0 a$ is the nonlocal parameter that describes the effect of small scale on the mechanical behavior. The parameter e_0 is a constant which has to be determined for each material independently and a is an internal characteristics length. Eringen (1983) estimated the parameter e_0 as 0.39. Several authors reported that the value of $e_0 a$ varies between 0 to 2 nm for analyzing carbon nanotubes (Sudak 2003, Wang and Hu 2005).

In cylindrical coordinates (r, θ, z), Eq. (2) can be rewritten as follows

$$\sigma_{rr}^{nl} - \gamma^2 (\nabla^2 \boldsymbol{\sigma}^{nl})_{rr} = \sigma_{rr}^l \tag{3}$$

$$\sigma_{\theta\theta}^{nl} - \gamma^2 (\nabla^2 \boldsymbol{\sigma}^{nl})_{\theta\theta} = \sigma_{\theta\theta}^l \tag{4}$$

$$\sigma_{r\theta}^{nl} - \gamma^2 (\nabla^2 \boldsymbol{\sigma}^{nl})_{r\theta} = \sigma_{r\theta}^l \tag{5}$$

$$\sigma_{rz}^{nl} - \gamma^2 (\nabla^2 \boldsymbol{\sigma}^{nl})_{rz} = \sigma_{rz}^l \tag{6}$$

$$\sigma_{\theta z}^{nl} - \gamma^2 (\nabla^2 \boldsymbol{\sigma}^{nl})_{\theta z} = \sigma_{\theta z}^l \tag{7}$$

$$\sigma_{zz}^{nl} - \gamma^2 (\nabla^2 \boldsymbol{\sigma}^{nl})_{zz} = \sigma_{zz}^l \tag{8}$$

The expressions for components of Laplacian of the symmetrical second order tensor are given by Povstenko (1995). Using these equations, the Laplacian of the nonlocal stress tensor $\boldsymbol{\sigma}^{nl}$ in cylindrical coordinates are obtained as follows

$$(\nabla^2 \boldsymbol{\sigma}^{nl})_{rr} = \nabla^2 \sigma_{rr}^{nl} - \frac{4}{r^2} \frac{\partial \sigma_{r\theta}^{nl}}{\partial \theta} - \frac{2}{r^2} (\sigma_{rr}^{nl} - \sigma_{\theta\theta}^{nl}) \tag{9}$$

$$(\nabla^2 \boldsymbol{\sigma}^{nl})_{\theta\theta} = \nabla^2 \sigma_{\theta\theta}^{nl} + \frac{4}{r^2} \frac{\partial \sigma_{r\theta}^{nl}}{\partial \theta} + \frac{2}{r^2} (\sigma_{rr}^{nl} - \sigma_{\theta\theta}^{nl}) \tag{10}$$

$$(\nabla^2 \boldsymbol{\sigma}^{nl})_{r\theta} = \nabla^2 \sigma_{r\theta}^{nl} - \frac{4}{r^2} \sigma_{r\theta}^{nl} + \frac{2}{r^2} \frac{\partial}{\partial \theta} (\sigma_{rr}^{nl} - \sigma_{\theta\theta}^{nl}) \tag{11}$$

$$(\nabla^2 \boldsymbol{\sigma}^{nl})_{rz} = \nabla^2 \sigma_{rz}^{nl} - \frac{1}{r^2} \sigma_{rz}^{nl} - \frac{2}{r^2} \frac{\partial \sigma_{\theta z}^{nl}}{\partial \theta} \tag{12}$$

$$(\nabla^2 \boldsymbol{\sigma}^{nl})_{\theta z} = \nabla^2 \sigma_{\theta z}^{nl} - \frac{1}{r^2} \sigma_{\theta z}^{nl} + \frac{2}{r^2} \frac{\partial \sigma_{rz}^{nl}}{\partial \theta} \tag{13}$$

$$(\nabla^2 \boldsymbol{\sigma}^{nl})_{zz} = \nabla^2 \sigma_{zz}^{nl} \tag{14}$$

where

$$\nabla^2 f = \frac{\partial^2 f}{\partial r^2} + \frac{1}{r} \frac{\partial f}{\partial r} + \frac{1}{r^2} \frac{\partial^2 f}{\partial \theta^2} + \frac{\partial^2 f}{\partial z^2} \tag{15}$$

The Frenet coordinate system is used in the formulation of problems of curved beams. The cylindrical and Frenet coordinate systems are given in Fig. 1. The stresses on a point A in the cross-section of the curved beam in Fig. 1 are given in the cylindrical coordinate system as $\sigma_{\theta\theta}$,
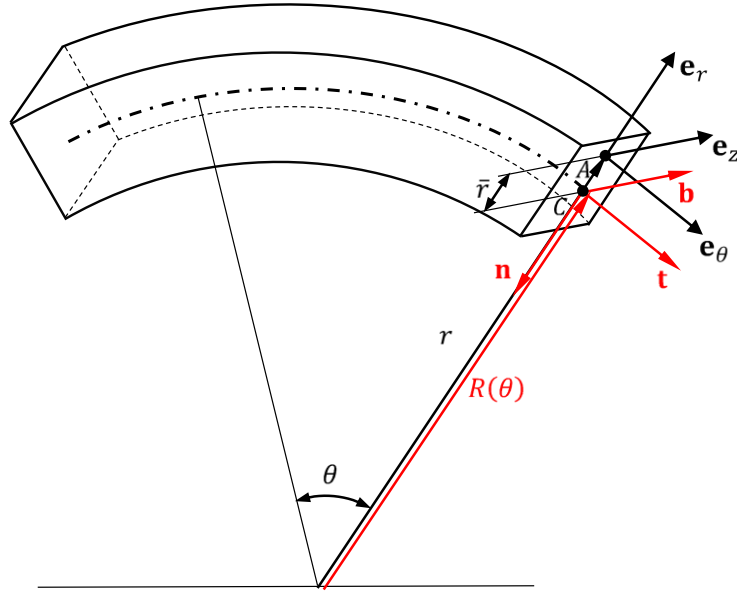
Fig. 1 The Frenet and cylindrical coordinates of a curved beam

$\sigma_{r\theta}$ and $\sigma_{\theta z}$. The normal stresses in radial direction σ_{rr} and in z direction σ_{zz} and also shear stress σ_{rz} are assumed as zero. For in-plane problems of planar curved beams, the normal stress in θ direction $\sigma_{\theta\theta}$ and the shear stress $\sigma_{r\theta}$ and their resultants F_n^{nl}, F_t^{nl} and M_b^{nl} are considered in the formulation. The relations between the stresses in Frenet and cylindrical coordinates are as follows

$$\sigma_n = -\sigma_{rr} = 0 \ ; \quad \sigma_b = \sigma_{zz} = 0 \ ; \quad \sigma_t = \sigma_{\theta\theta} \neq 0 \tag{16}$$

$$\sigma_{nt} = -\sigma_{r\theta} \neq 0 \ ; \quad \sigma_{tb} = \sigma_{\theta z} \neq 0 \ ; \quad \sigma_{nb} = -\sigma_{rz} = 0 \tag{17}$$

$R(\theta)$ is the curvature of the centroid of the cross-section (point C), and $\bar{r}$ is the coordinate of an arbitrary point A shown in Fig. 1. Since a uniform circular beam is considered in this study, the radius of the beam is constant, i.e., $R(\theta) = R$, and the coordinate r is described as

$$r = R + \bar{r} \qquad\qquad \partial r = \partial \bar{r} \tag{18}$$

It is assumed that $\bar{r}/R \ll 1$ (beam assumption).

$F_n^{nl}(\theta)$, $F_t^{nl}(\theta)$ and $M_b^{nl}(\theta)$ are the stress resultants of the cross-section at the coordinate θ and depend on only the coordinate θ. Thus, their derivatives with respect to the coordinate θ are non-zero and derivatives with respect to the coordinates $\bar{r}$ and z are zero.

The equilibrium equations (without body forces) in cylindrical coordinates are known as

$$\frac{\partial \sigma_{rr}^{nl}}{\partial r} + \frac{\sigma_{rr}^{nl} - \sigma_{\theta\theta}^{nl}}{r} + \frac{1}{r}\frac{\partial \sigma_{r\theta}^{nl}}{\partial \theta} + \frac{\partial \sigma_{rz}^{nl}}{\partial z} = 0 \tag{19}$$

$$\frac{\partial \sigma_{r\theta}^{nl}}{\partial r} + \frac{2\sigma_{r\theta}^{nl}}{r} + \frac{1}{r}\frac{\partial \sigma_{\theta\theta}^{nl}}{\partial \theta} + \frac{\partial \sigma_{\theta z}^{nl}}{\partial z} = 0 \tag{20}$$

$$\frac{\partial \sigma_{zr}^{nl}}{\partial r} + \frac{\sigma_{zr}^{nl}}{r} + \frac{1}{r}\frac{\partial \sigma_{z\theta}^{nl}}{\partial \theta} + \frac{\partial \sigma_{zz}^{nl}}{\partial z} = 0 \tag{21}$$

The equilibrium equations can be rewritten in the following form by using the Eqs. (16)-(17)

$$-\frac{1}{r}\sigma_{\theta\theta}^{nl} + \frac{1}{r}\frac{\partial \sigma_{r\theta}^{nl}}{\partial \theta} = 0 \tag{22}$$

$$\frac{\partial \sigma_{r\theta}^{nl}}{\partial \bar{r}} + \frac{1}{r}2\sigma_{r\theta}^{nl} + \frac{1}{r}\frac{\partial \sigma_{\theta\theta}^{nl}}{\partial \theta} + \frac{\partial \sigma_{\theta z}^{nl}}{\partial z} = 0 \tag{23}$$

$$\frac{1}{r}\frac{\partial \sigma_{z\theta}^{nl}}{\partial \theta} = 0 \tag{24}$$

Eq. (3) is arranged by substituting Eq. (9) and Eq. (15) for σ_{rr}^{nl} in the following form

$$\sigma_{rr}^{nl} - \gamma^2 \left[\left(\frac{\partial^2 \sigma_{rr}^{nl}}{\partial \bar{r}^2} + \frac{1}{r}\frac{\partial \sigma_{rr}^{nl}}{\partial \bar{r}} + \frac{1}{r^2}\frac{\partial^2 \sigma_{rr}^{nl}}{\partial \theta^2} + \frac{\partial^2 \sigma_{rr}^{nl}}{\partial z^2}\right) - \frac{4}{r^2}\frac{\partial \sigma_{r\theta}^{nl}}{\partial \theta} - \frac{2}{r^2}\left(\sigma_{rr}^{nl} - \sigma_{\theta\theta}^{nl}\right)\right] = \sigma_{rr}^l \tag{25}$$

by using the beam assumptions, i.e. Eqs. (16-17)

$$-\frac{4}{r^2}\frac{\partial \sigma_{r\theta}^{nl}}{\partial \theta} + \frac{2}{r^2}\sigma_{\theta\theta}^{nl} = 0 \tag{26}$$

is obtained.

Substituting Eq. (10) and Eq. (15) for $\sigma_{\theta\theta}^{nl}$ into Eq. (4) yields

$$\sigma_{\theta\theta}^{nl} - \gamma^2 \left[\left(\frac{\partial^2 \sigma_{\theta\theta}^{nl}}{\partial \bar{r}^2} + \frac{1}{r}\frac{\partial \sigma_{\theta\theta}^{nl}}{\partial \bar{r}} + \frac{1}{r^2}\frac{\partial^2 \sigma_{\theta\theta}^{nl}}{\partial \theta^2} + \frac{\partial^2 \sigma_{\theta\theta}^{nl}}{\partial z^2}\right) + \frac{4}{r^2}\frac{\partial \sigma_{r\theta}^{nl}}{\partial \theta} + \frac{2}{r^2}\left(\sigma_{rr}^{nl} - \sigma_{\theta\theta}^{nl}\right)\right] = \sigma_{\theta\theta}^l \tag{27}$$

By using Eqs. (16)-(17), previous relation simplifies to

$$\sigma_{\theta\theta}^{nl} - \gamma^2 \left[\left(\frac{\partial^2 \sigma_{\theta\theta}^{nl}}{\partial \bar{r}^2} + \frac{1}{r}\frac{\partial \sigma_{\theta\theta}^{nl}}{\partial \bar{r}} + \frac{1}{r^2}\frac{\partial^2 \sigma_{\theta\theta}^{nl}}{\partial \theta^2} + \frac{\partial^2 \sigma_{\theta\theta}^{nl}}{\partial z^2}\right) + \frac{4}{r^2}\frac{\partial \sigma_{r\theta}^{nl}}{\partial \theta} - \frac{2}{r^2}\sigma_{\theta\theta}^{nl}\right] = \sigma_{\theta\theta}^l \tag{28}$$

Substituting Eq. (26) into Eq. (28), the following is obtained

$$\sigma_{\theta\theta}^{nl} - \gamma^2 \left[\left(\frac{\partial^2 \sigma_{\theta\theta}^{nl}}{\partial \bar{r}^2} + \frac{1}{r}\frac{\partial \sigma_{\theta\theta}^{nl}}{\partial \bar{r}} + \frac{1}{r^2}\frac{\partial^2 \sigma_{\theta\theta}^{nl}}{\partial \theta^2} + \frac{\partial^2 \sigma_{\theta\theta}^{nl}}{\partial z^2}\right)\right] = \sigma_{\theta\theta}^l \tag{29}$$

Eq. (5) can be arranged by substituting Eq. (11) and Eq. (15) for $\sigma_{r\theta}^{nl}$ as follows

$$\sigma_{r\theta}^{nl} - \gamma^2 \left[\left(\frac{\partial^2 \sigma_{r\theta}^{nl}}{\partial \bar{r}^2} + \frac{1}{r}\frac{\partial \sigma_{r\theta}^{nl}}{\partial \bar{r}} + \frac{1}{r^2}\frac{\partial^2 \sigma_{r\theta}^{nl}}{\partial \theta^2} + \frac{\partial^2 \sigma_{r\theta}^{nl}}{\partial z^2}\right) - \frac{4}{r^2}\sigma_{r\theta}^{nl} + \frac{2}{r^2}\frac{\partial}{\partial \theta}\left(\sigma_{rr}^{nl} - \sigma_{\theta\theta}^{nl}\right)\right] = \sigma_{r\theta}^l \tag{30}$$

By using Eqs. (16)-(17)

$$\sigma_{r\theta}^{nl} - \gamma^2 \left[\left(\frac{\partial^2 \sigma_{r\theta}^{nl}}{\partial \bar{r}^2} + \frac{1}{r}\frac{\partial \sigma_{r\theta}^{nl}}{\partial \bar{r}} + \frac{1}{r^2}\frac{\partial^2 \sigma_{r\theta}^{nl}}{\partial \theta^2} + \frac{\partial^2 \sigma_{r\theta}^{nl}}{\partial z^2}\right) - \frac{4}{r^2}\sigma_{r\theta}^{nl} - \frac{2}{r^2}\frac{\partial \sigma_{\theta\theta}^{nl}}{\partial \theta}\right] = \sigma_{r\theta}^l \tag{31}$$

is obtained.

The relation between the local and nonlocal stress resultants F_t^l and F_t^{nl} can be obtained by integrating Eq. (29) over the cross-section.

$$\iint_A \left[\sigma_{\theta\theta}^{nl} - \gamma^2 \left[\left(\frac{\partial^2 \sigma_{\theta\theta}^{nl}}{\partial \bar{r}^2} + \frac{1}{r} \frac{\partial \sigma_{\theta\theta}^{nl}}{\partial \bar{r}} + \frac{1}{r^2} \frac{\partial^2 \sigma_{\theta\theta}^{nl}}{\partial \theta^2} + \frac{\partial^2 \sigma_{\theta\theta}^{nl}}{\partial z^2} \right) \right] \right] dA = \iint_A [\sigma_{\theta\theta}^l] dA \tag{32}$$

Substituting Eq. (18) into this equation yields

$$\iint_A \left[\sigma_{\theta\theta}^{nl} - \gamma^2 \left[\left(\frac{\partial^2 \sigma_{\theta\theta}^{nl}}{\partial \bar{r}^2} + \frac{1}{R+\bar{r}} \frac{\partial \sigma_{\theta\theta}^{nl}}{\partial \bar{r}} + \frac{1}{(R+\bar{r})^2} \frac{\partial^2 \sigma_{\theta\theta}^{nl}}{\partial \theta^2} + \frac{\partial^2 \sigma_{\theta\theta}^{nl}}{\partial z^2} \right) \right] \right] dA = \iint_A [\sigma_{\theta\theta}^l] dA \tag{33}$$

The following is obtained by assuming $\bar{r}/R \ll 1$ (beam assumption).

$$\iint_A [\sigma_{\theta\theta}^{nl}] dA - \gamma^2 \iint_A \frac{\partial^2 \sigma_{\theta\theta}^{nl}}{\partial \bar{r}^2} dA - \gamma^2 \frac{1}{R} \iint_A \frac{\partial \sigma_{\theta\theta}^{nl}}{\partial \bar{r}} dA - \gamma^2 \frac{1}{R^2} \iint_A \frac{\partial^2 \sigma_{\theta\theta}^{nl}}{\partial \theta^2} dA$$
$$- \gamma^2 \iint_A \frac{\partial^2 \sigma_{\theta\theta}^{nl}}{\partial z^2} dA = \iint_A [\sigma_{\theta\theta}^l] dA \tag{34}$$

By using Leibniz integral rule (Abramowitz and Stegun 1972), Eq. (34) can be expressed as

$$\iint_A \sigma_{\theta\theta}^{nl} dA - \gamma^2 \frac{\partial^2}{\partial \bar{r}^2} \iint_A \sigma_{\theta\theta}^{nl} dA - \gamma^2 \frac{1}{R} \frac{\partial}{\partial \bar{r}} \iint_A \sigma_{\theta\theta}^{nl} dA - \gamma^2 \frac{1}{R^2} \frac{\partial^2}{\partial \theta^2} \iint_A \sigma_{\theta\theta}^{nl} dA$$
$$- \gamma^2 \frac{\partial^2}{\partial z^2} \iint_A \sigma_{\theta\theta}^{nl} dA = \iint_A \sigma_{\theta\theta}^l dA \tag{35}$$

where

$$\iint_A \sigma_{\theta\theta}^{nl} dA = F_t^{nl} \qquad\qquad \iint_A \sigma_{\theta\theta}^l dA = F_t^l \tag{36}$$

By substituting Eq. (36) into the Eq. (35)

$$F_t^{nl} - \gamma^2 \frac{\partial^2 F_t^{nl}}{\partial \bar{r}^2} - \gamma^2 \frac{1}{R} \frac{\partial F_t^{nl}}{\partial \bar{r}} - \frac{\gamma^2}{R^2} \frac{\partial^2 F_t^{nl}}{\partial \theta^2} - \gamma^2 \frac{\partial^2 F_t^{nl}}{\partial z^2} = F_t^l \tag{37}$$

is obtained. Eq. (37) can be arranged by remembering the only non-zero derivatives are with respect to θ and other derivatives are zero

$$F_t^{nl} - \frac{\gamma^2}{R^2} \frac{\partial^2 F_t^{nl}}{\partial \theta^2} = F_t^l \tag{38}$$

Similarly; integrating Eq. (31) over the beam cross-section gives the relation between the local and nonlocal stress resultants F_n^l and F_n^{nl}

$$\iint_A \left[\sigma_{r\theta}^{nl} - \gamma^2 \left[\left(\frac{\partial^2 \sigma_{r\theta}^{nl}}{\partial \bar{r}^2} + \frac{1}{r} \frac{\partial \sigma_{r\theta}^{nl}}{\partial \bar{r}} + \frac{1}{r^2} \frac{\partial^2 \sigma_{r\theta}^{nl}}{\partial \theta^2} + \frac{\partial^2 \sigma_{r\theta}^{nl}}{\partial z^2} \right) - \frac{4}{r^2} \sigma_{r\theta}^{nl} - \frac{2}{r^2} \frac{\partial \sigma_{\theta\theta}^{nl}}{\partial \theta} \right] \right] dA$$
$$= \iint_A \sigma_{r\theta}^l dA \tag{39}$$

Eq. (23) can be rewritten in the following form

$$\frac{\partial \sigma_{r\theta}^{nl}}{\partial r} + \frac{\partial \sigma_{\theta z}^{nl}}{\partial z} = -\frac{2\sigma_{r\theta}^{nl}}{r} - \frac{1}{r}\frac{\partial \sigma_{\theta\theta}^{nl}}{\partial \theta} \tag{40}$$

Substituting Eq. (40) into Eq. (39) yields

$$\iint_A \left[\sigma_{r\theta}^{nl} - \gamma^2 \left[\left(\frac{\partial^2 \sigma_{r\theta}^{nl}}{\partial \bar{r}^2} + \frac{1}{r}\frac{\partial \sigma_{r\theta}^{nl}}{\partial \bar{r}} + \frac{1}{r^2}\frac{\partial^2 \sigma_{r\theta}^{nl}}{\partial \theta^2} + \frac{\partial^2 \sigma_{r\theta}^{nl}}{\partial z^2} \right) + \frac{2}{r}\frac{\partial \sigma_{r\theta}^{nl}}{\partial \bar{r}} + \frac{2}{r}\frac{\partial \sigma_{\theta z}^{nl}}{\partial z} \right] \right] dA$$
$$= \iint_A \sigma_{r\theta}^l dA \tag{41}$$

Substituting Eq. (18) into this equation and assuming $\bar{r}/R \ll 1$ (beam assumption) gives the following equation

$$\iint_A \sigma_{r\theta}^{nl} dA - \gamma^2 \iint_A \frac{\partial^2 \sigma_{r\theta}^{nl}}{\partial \bar{r}^2} dA - \gamma^2 \frac{1}{R} \iint_A \frac{\partial \sigma_{r\theta}^{nl}}{\partial r} dA - \gamma^2 \frac{1}{R^2} \iint_A \frac{\partial^2 \sigma_{r\theta}^{nl}}{\partial \theta^2} dA$$
$$- \gamma^2 \iint_A \frac{\partial^2 \sigma_{r\theta}^{nl}}{\partial z^2} dA - \gamma^2 \frac{2}{R} \iint_A \frac{\partial \sigma_{r\theta}^{nl}}{\partial \bar{r}} dA - \gamma^2 \frac{2}{R} \iint_A \frac{\partial \sigma_{\theta z}^{nl}}{\partial z} dA = \iint_A \sigma_{r\theta}^l dA \tag{42}$$

By using Leibniz integral rule and the definitions

$$\iint_A \sigma_{r\theta}^{nl} dA = -F_n^{nl} \qquad \iint_A \sigma_{r\theta}^l dA = -F_n^l \qquad \iint_A \sigma_{\theta z}^{nl} dA = F_b^{nl} \tag{43}$$

One can obtain the following expression by remembering the only non-zero derivatives are with respect to θ and others are zero

$$F_n^{nl} - \frac{\gamma^2}{R^2}\frac{\partial^2 F_n^{nl}}{\partial \theta^2} = F_n^l \tag{44}$$

Multiplying both sides of Eq. (29) with coordinate $\bar{r}$ and integrating the resulting expression over the beam cross-section yields the relation between the local and nonlocal stress resultants M_b^l and M_b^{nl}

$$\iint_A \left\{ \sigma_{\theta\theta}^{nl} - \gamma^2 \left[\left(\frac{\partial^2 \sigma_{\theta\theta}^{nl}}{\partial \bar{r}^2} + \frac{1}{r}\frac{\partial \sigma_{\theta\theta}^{nl}}{\partial \bar{r}} + \frac{1}{r^2}\frac{\partial^2 \sigma_{\theta\theta}^{nl}}{\partial \theta^2} + \frac{\partial^2 \sigma_{\theta\theta}^{nl}}{\partial z^2} \right) \right] \right\} \bar{r} dA = \iint_A \sigma_{\theta\theta}^l \bar{r} dA \tag{45}$$

Using integration by parts as given in the following equation

$$\iint_A \frac{\partial}{\partial z}[f_r(\bar{r},z)]g(\bar{r},z)dA = \iint_A \left\{ \frac{\partial}{\partial z}[f(\bar{r},z)g(\bar{r},z)] - f(\bar{r},z)\frac{\partial}{\partial z}[g(\bar{r},z)] \right\} dA \tag{46}$$

and also using Leibniz integral rule, Eq. (45) can be arranged in the following form

$$\iint_A \sigma_{\theta\theta}^{nl} \bar{r} dA - \gamma^2 \frac{\partial^2}{\partial \bar{r}^2} \iint_A [\sigma_{\theta\theta}^{nl}\bar{r}]dA + 2\gamma^2 \frac{\partial}{\partial \bar{r}} \iint_A \sigma_{\theta\theta}^{nl} dA - \frac{\gamma^2}{R}\frac{\partial}{\partial \bar{r}} \iint_A [\sigma_{\theta\theta}^{nl}\bar{r}]dA$$
$$+ \frac{\gamma^2}{R} \iint_A \sigma_{\theta\theta}^{nl} dA - \frac{\gamma^2}{R^2}\frac{\partial^2}{\partial \theta^2} \iint_A \sigma_{\theta\theta}^{nl} \bar{r} dA - \gamma^2 \frac{\partial^2}{\partial z^2} \iint_A \sigma_{\theta\theta}^{nl} \bar{r} dA = \iint_A \sigma_{\theta\theta}^l \bar{r} dA \tag{47}$$
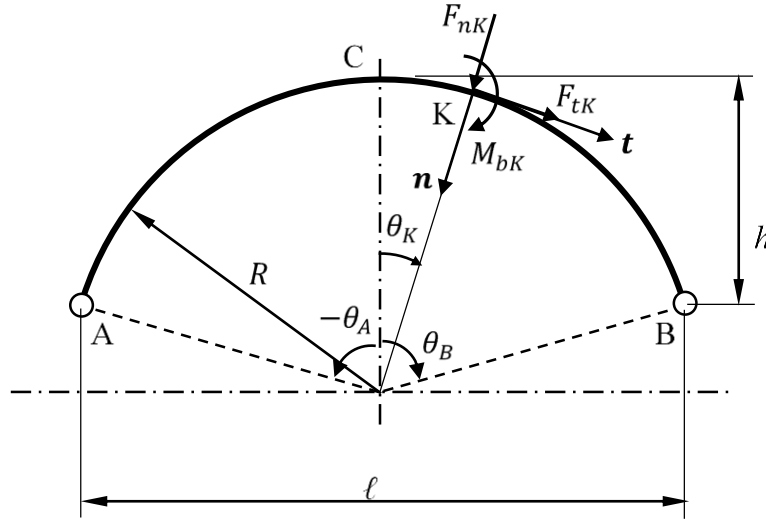
Fig. 2 Circular beam with nonsymmetrical boundary and loading conditions

where

$$\iint_A \sigma_{\theta\theta}^{nl} \bar{r} dA = M_b^{nl} \qquad \iint_A \sigma_{\theta\theta}^{l} \bar{r} dA = M_b^{l} \qquad \iint_A \sigma_{\theta\theta}^{l} dA = F_t^{l} \qquad (48)$$

By substituting Eq. (48) into the Eq. (47) and remembering the only non-zero derivatives are with respect to θ and others are zero, the following expression is obtained

$$M_b^{nl} - \frac{\gamma^2}{R^2}\frac{\partial^2 M_b^{nl}}{\partial\theta^2} + \frac{\gamma^2}{R}F_t^{nl} = M_b^{l} \qquad (49)$$

In local elasticity theory, the governing equations of in-plane static behavior of a circular uniform beam under concentrated loads (Fig. 2), considering the effects of axial extension and shear deformation, are very well-known as (Tufekci and Arpaci 2006)

$$\frac{dw(\theta)}{d\theta} = u(\theta) + \frac{R}{EA}F_t^{l}(\theta) \qquad (50)$$

$$\frac{du(\theta)}{d\theta} = -w(\theta) + \frac{k_n R F_n^{l}(\theta)}{GA} + R\Omega_b(\theta) \qquad (51)$$

$$\frac{d\Omega_b(\theta)}{d\theta} = \frac{R}{EI_b}M_b^{l}(\theta) \qquad (52)$$

$$\frac{dM_b^{l}(\theta)}{d\theta} = -RF_n^{l}(\theta) \qquad (53)$$

$$\frac{dF_t^{l}(\theta)}{d\theta} = F_n^{l}(\theta) \qquad (54)$$

$$\frac{dF_n^l(\theta)}{d\theta} = -F_t^l(\theta) \tag{55}$$

where u and w are the normal and tangential displacements, Ω_b is the rotation angle about the binormal axis, θ is the angular coordinate; R is the radius of curvature of the beam; A is the cross-sectional area; I_b is the area moment of inertia of the cross-section with respect to the binormal axis; k_n is the factor of shear distribution along the normal axis; F_n^l and F_t^l are normal and tangential components of internal force, respectively; M_b^l is the internal moment about the binormal axis; E and G are respectively Young's and shear moduli. In this study, a circular beam with uniform doubly symmetric cross-section is considered.

The equilibrium Eqs. (53)-(55) are also valid in nonlocal elasticity and differentiated with respect to the angular coordinate θ, and they are substituted into Eqs. (38), (44) and (49). Then, the obtained equations are substituted into the Eqs. (50)-(52) and the governing differential equations of nonlocal beams can be rewritten in the following form

$$\frac{dw(\theta)}{d\theta} = u(\theta) + \frac{R}{EA}\left(1 + \frac{\gamma^2}{R^2}\right)F_t^{nl}(\theta) \tag{56}$$

$$\frac{du(\theta)}{d\theta} = -w(\theta) + R\Omega_b(\theta) + \frac{k_n R}{GA}\left(1 + \frac{\gamma^2}{R^2}\right)F_n^{nl}(\theta) \tag{57}$$

$$\frac{d\Omega_b(\theta)}{d\theta} = \frac{R}{EI_b}M_b^{nl}(\theta) \tag{58}$$

$$\frac{dM_b^{nl}(\theta)}{d\theta} = -RF_n^{nl}(\theta) \tag{59}$$

$$\frac{dF_t^{nl}(\theta)}{d\theta} = F_n^{nl}(\theta) \tag{60}$$

$$\frac{dF_n^{nl}(\theta)}{d\theta} = -F_t^{nl}(\theta) \tag{61}$$

Equations can also be stated in the matrix form as

$$\frac{d\mathbf{y}(\theta)}{d\theta} = \mathbf{A}(\theta)\mathbf{y}(\theta) \tag{62}$$

where $\mathbf{y}(\theta)$ is the vector of variables, namely, w, u, Ω_b, M_b^{nl}, F_t^{nl}, F_n^{nl}, $\mathbf{A}(\theta)$ is the 6×6 coefficient matrix. The solution of the Eq. (62) can be expressed as

$$\mathbf{y}(\theta) = \mathbf{Y}(\theta, \theta_0)\mathbf{y}_o \tag{63}$$

where $\mathbf{Y}(\theta, \theta_0)$ is the fundamental matrix; $\mathbf{y}_0 = \mathbf{y}(\theta_0)$ is the vector of initial values at the coordinate θ_0 (in this study $\theta_0 = 0$).

The solution of this equation can be written in the following form

$$\begin{bmatrix} w(\theta) \\ u(\theta) \\ \Omega_b(\theta) \\ M_b^{nl}(\theta) \\ F_t^{nl}(\theta) \\ F_n^{nl}(\theta) \end{bmatrix} = \begin{bmatrix} Y_{11} & Y_{12} & Y_{13} & Y_{14} & Y_{15} & Y_{16} \\ Y_{21} & Y_{22} & Y_{23} & Y_{24} & Y_{25} & Y_{26} \\ Y_{31} & Y_{32} & Y_{33} & Y_{34} & Y_{35} & Y_{36} \\ Y_{41} & Y_{42} & Y_{43} & Y_{44} & Y_{45} & Y_{46} \\ Y_{51} & Y_{52} & Y_{53} & Y_{54} & Y_{55} & Y_{56} \\ Y_{61} & Y_{62} & Y_{63} & Y_{64} & Y_{65} & Y_{66} \end{bmatrix} \begin{bmatrix} w_0 \\ u_0 \\ \Omega_{b0} \\ M_{b0}^{nl} \\ F_{t0}^{nl} \\ F_{n0}^{nl} \end{bmatrix} \tag{64}$$

The fundamental matrix satisfies the following requirements

$$\frac{d\mathbf{Y}(\theta,\theta_0)}{d\theta} = \mathbf{A}(\theta)\mathbf{Y}(\theta,\theta_0), \qquad \mathbf{Y}(\theta_0,\theta_0) = \mathbf{I}$$

$$\mathbf{Y}(\theta_1,\theta_2)\mathbf{Y}(\theta_2,\theta_3) = \mathbf{Y}(\theta_1,\theta_3), \qquad \mathbf{Y}(\theta_1,\theta_2) = \mathbf{Y}^{-1}(\theta_2,\theta_1) \tag{65}$$

where $\mathbf{I}$ is the unit matrix.

The exact analytical solution of the differential equations and the fundamental matrix of a circular uniform nanobeam can be obtained easily in the following form

$$Y_{11} = \cos\theta \tag{66}$$

$$Y_{12} = \sin\theta \tag{67}$$

$$Y_{13} = R(1 - \cos\theta) \tag{68}$$

$$Y_{14} = \frac{R^2(\theta - \sin\theta)}{EI_b} \tag{69}$$

$$Y_{15} = \frac{R^3}{EI_b}\left(\theta - \frac{3\sin\theta}{2} + \frac{\theta\cos\theta}{2}\right) + \frac{R}{2EA}(\theta\cos\theta + \sin\theta)\left(1 + \frac{\gamma^2}{R^2}\right)$$
$$+ \frac{k_n R}{2GA}(\theta\cos\theta - \sin\theta)\left(1 + \frac{\gamma^2}{R^2}\right) \tag{70}$$

$$Y_{16} = -\frac{R^3}{EI_b}\left(1 - \cos\theta - \frac{\theta\sin\theta}{2}\right) + \frac{R\theta\sin\theta}{2EA}\left(1 + \frac{\gamma^2}{R^2}\right) + \frac{k_n R\theta\sin\theta}{2GA}\left(1 + \frac{\gamma^2}{R^2}\right) \tag{71}$$

$$Y_{21} = -\sin\theta \tag{72}$$

$$Y_{22} = \cos\theta \tag{73}$$

$$Y_{23} = R_0\sin\theta \tag{74}$$

$$Y_{24} = \frac{2R^2}{EI_b}\left(\sin\frac{\theta}{2}\right)^2 \tag{75}$$

$$Y_{25} = \frac{R^3}{EI_b}\left(1 - \cos\theta - \frac{\theta\sin\theta}{2}\right) - \frac{R\theta\sin\theta}{2EA}\left(1 + \frac{\gamma^2}{R^2}\right) - \frac{k_n R\theta\sin\theta}{2GA}\left(1 + \frac{\gamma^2}{R^2}\right) \tag{76}$$

$$Y_{26} = \frac{R^3}{2EI_b}(\theta \cos \theta - \sin \theta) + \frac{R}{2EA}(\theta \cos \theta - \sin \theta)\left(1 + \frac{\gamma^2}{R^2}\right)$$
$$+ \frac{k_n R}{2GA}(\theta \cos \theta + \sin \theta)\left(1 + \frac{\gamma^2}{R^2}\right) \tag{77}$$

$$Y_{33} = 1 \tag{78}$$

$$Y_{34} = \frac{R\theta}{EI_b} \tag{79}$$

$$Y_{35} = \frac{R^2}{EI_b}(\theta - \sin \theta) \tag{80}$$

$$Y_{36} = -\frac{2R^2}{EI_b}\left(\sin \frac{\theta}{2}\right)^2 \tag{81}$$

$$Y_{44} = 1 \tag{82}$$

$$Y_{45} = R(1 - \cos \theta) \tag{83}$$

$$Y_{46} = -R \sin \theta \tag{84}$$

$$Y_{55} = \cos \theta \tag{85}$$

$$Y_{56} = \sin \theta \tag{86}$$

$$Y_{65} = -\sin \theta \tag{87}$$

$$Y_{66} = \cos \theta \tag{88}$$

All other terms of the fundamental matrix are zero. The inverse of the fundamental matrix can also be obtained analytically and it is not given here for the brevity.

If the initial values w_0, u_0, Ω_{b0}, M_{b0}^{nl}, F_{t0}^{nl}, F_{n0}^{nl}, are known, the solution are obtained analytically. The initial values are solved from a system of linear equations obtained from boundary conditions.

The classical boundary conditions are known as:

1- Hinged End: $w_A = 0$, $u_A = 0$, $M_{bA}^{nl} = 0$.
2- Clamped End: $w_A = 0$, $u_A = 0$, $\Omega_{bA} = 0$.
3- Free End: $M_{bA}^{nl} = 0$, $F_{tA}^{nl} = 0$, $F_{nA}^{nl} = 0$.

In this study, as a general case, a beam with point loads at the coordinate ($\theta = \theta_K$) is considered (Fig. 2). The beam has two regions and the solutions for both regions are

$$\mathbf{y}_1(\theta_1) = \mathbf{Y}(\theta_1, \theta_0)\mathbf{y}_{10} \qquad \text{for} \qquad -\theta_A \le \theta_1 \le \theta_K \tag{89}$$

$$\mathbf{y}_2(\theta_2) = \mathbf{Y}(\theta_2, \theta_K)\mathbf{y}_{2K} \qquad \text{for} \qquad \theta_K \le \theta_2 \le \theta_B \tag{90}$$

where $\mathbf{y}_{2K}$ is the vector of initial values for the second region at coordinate θ_K. The continuity condition at that point is

$$\mathbf{y}_1(\theta_K) - \mathbf{K} = \mathbf{y}_{2K} \tag{91}$$

where $\mathbf{K} = [0 \quad 0 \quad 0 \quad M_{Kb} \quad F_{Kt} \quad F_{Kn}]^{\mathrm{T}}$ is loading vector. Thus, Eq. (90) is rewritten as

$$\mathbf{y}_2(\theta_2) = \mathbf{Y}(\theta_2, \theta_K)\mathbf{y}_1(\theta_K) - \mathbf{Y}(\theta_2, \theta_K)\mathbf{K} \tag{92}$$

Substituting Eq. (89) into Eq. (92)

$$\mathbf{y}_2(\theta_2) = \mathbf{Y}(\theta_2, \theta_K)\mathbf{Y}(\theta_K, \theta_0)\mathbf{y}_{10} - \mathbf{Y}(\theta_2, \theta_K)\mathbf{K} \tag{93}$$

Using Eq. (65), Eq. (93) can be arranged as follows

$$\mathbf{y}_2(\theta_2) = \mathbf{Y}(\theta_2, \theta_0)\mathbf{y}_{10} - \mathbf{Y}(\theta_2, \theta_0)\,\mathbf{Y}^{-1}(\theta_K, \theta_0)\mathbf{K} \tag{94}$$

Thus, the unknown initial values are solved by using three simultaneous linear equations for each end. Now, it is possible to specify analytically the displacements, rotation, and internal forces and bending moment of the beam.

3. Numerical evaluation

In this section, several geometries, boundary and loading conditions are considered for numerical examples. These include hinged-hinged, clamped-clamped, hinged-clamped and clamped-free ends as boundary conditions; point loads in normal direction (normal force, F_n), tangential direction (tangential force, F_t) and binormal direction (bending moment, M_b) as loading types. The loads are applied at any coordinate θ_K. The slenderness ratio of the beam $\lambda = R\,\theta_t/\sqrt{I/A}$ is changed from 20 to 150 and the cross-section of the beam is considered as circular. Opening angle of the beam (θ_t) is taken as between 10° and 180°. Various problems are solved and the exact analytical equations of the displacements, rotation and the stress resultants are obtained. The effects of nanoscale parameter and variation of geometric parameters on the static behavior of a circular nanobeam analyzed and discussed through the proposed method. Small scale parameter (R/γ) is considered to change from 1 to 10 and γ is taken as 1.56 nm. Poisson's ratio and Young's modulus is taken as $\upsilon = 0.3$ and $E = 1\,TPa$, respectively. These values are taken from Hu *et al.* (2009), however, in this study the results do not depend on these values, since they are given as ratio of the results of local and nonlocal theories. The effects of axial extension, shear deformation and their nonlocal effects, along with the nonlocal effects of bending (binormal) moment are included in the equations. The results are presented for four different cases, in which (i) all effects are considered, (ii) only axial extension effect is considered, (iii) only shear deformation effect is considered, and (iv) none of the effects are considered.

3.1 A quarter circular beam with a tip force

In this example, a quarter circular cantilever nanobeam loaded with a normal force F_0 at the free end is considered (Fig. 3). The normal and tangential displacements and the rotation angle at the free end B are obtained analytically as follows

$$w_B = \left(\frac{F_0 k_n R}{2GA} - \frac{F_0 R}{2EA}\right)\left(1 + \frac{\gamma^2}{R^2}\right) + \frac{F_0 R^3}{2EI_b} \tag{95}$$
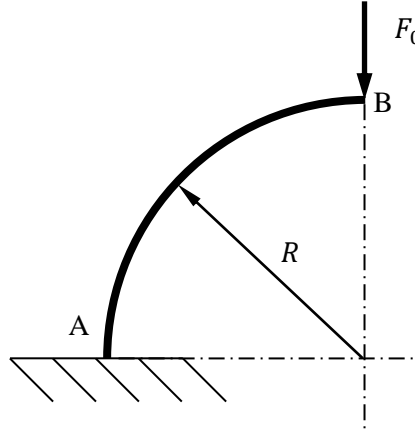
Fig. 3 A quarter circular cantilever beam with a tip force

$$u_B = \left(\frac{F_0 k_n \pi R}{4GA} + \frac{F_0 \pi R}{4EA}\right)\left(1 + \frac{\gamma^2}{R^2}\right) + \frac{F_0 \pi R^3}{4EI_b} \tag{96}$$

$$\Omega_{bB} = \frac{F_0 R^2}{EI_b} \tag{97}$$

As seen from these equations, the nonlocal parameter γ/R is important for a very small radius of curvature. The results of the classical (local) theory can be obtained by cancelling out the term γ/R.

Functions of tangential displacement $w = w(\theta)$, normal displacement $u = u(\theta)$ and rotation angle $\Omega_b = \Omega_b(\theta)$ can be obtained as follows

$$w(\theta) = \left(\frac{F_0 k_n R}{2GA} - \frac{F_0 R}{2EA}\right)\left(1 + \frac{\gamma^2}{R^2}\right)\cos\theta + \left(\frac{F_0 k_n R}{2GA} + \frac{F_0 R}{2EA}\right)\left(\frac{\pi}{2} + \theta\right)\left(1 + \frac{\gamma^2}{R^2}\right)\sin\theta$$
$$+ \frac{F_0 R^3}{2EI_b}\left[\left(\frac{\pi}{2} + \theta\right)\sin\theta + \cos\theta\right] \tag{98}$$

$$u(\theta) = \left(\frac{F_0 R}{2EA} + \frac{F_0 k_n R}{2GA}\right)\left(\frac{\pi}{2} + \theta\right)\left(1 + \frac{\gamma^2}{R^2}\right)\cos\theta + \frac{F_0 R^3}{2EI_b}\left(\frac{\pi}{2} + \theta\right)\cos\theta \tag{99}$$

$$\Omega_b(\theta) = \frac{F_0 R^2}{EI_b}\cos\theta \tag{100}$$

3.2 Pinched nanoring

In this example, static behavior of a pinched circular ring (Fig. 4) is studied. These structures are observed in experimental studies (Kong *et al.* 2004, Huang *et al.* 2012).

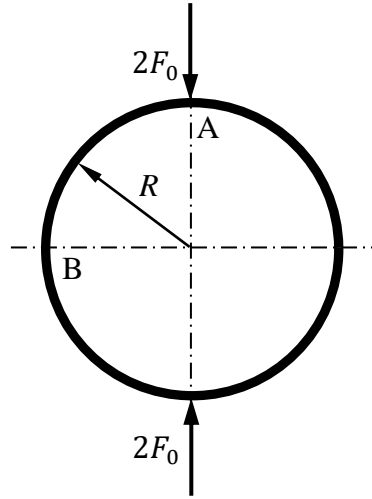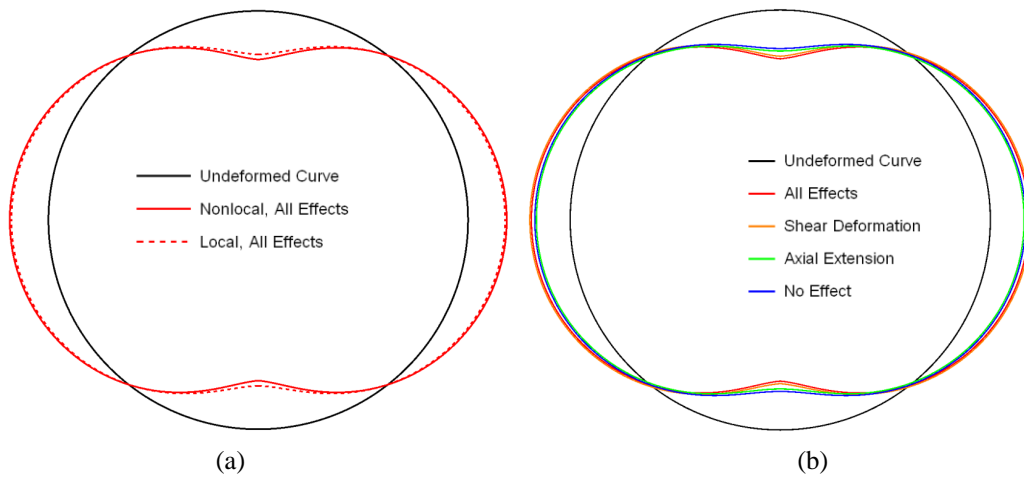The normal displacements at points A and B are obtained as

Fig. 4 Circular nanoring with concentrated forces

(a)   (b)

Fig. 5 The displacement diagram for the nanoring obtained (a) by local and nonlocal theories (b) nonlocal theory considering the effects ($\lambda = 20$ and $R/\gamma = 1$)

$$u_A = \frac{F_0 R^3}{EI_b}\left(\frac{\pi}{4} - \frac{2}{\pi}\right) + \left(\frac{F_0 \pi R}{4EA} + \frac{F_0 k_n \pi R}{4GA}\right)\left(1 + \frac{\gamma^2}{R^2}\right) \qquad (101)$$

$$u_B = \left(\frac{F_0 R^3}{2EI_b} - \frac{2F_0 R^3}{\pi EI_b}\right) + \left(\frac{F_0 R}{2EA} - \frac{F_0 k_n R}{2GA}\right)\left(1 + \frac{\gamma^2}{R^2}\right) \qquad (102)$$

and the moments are

$$M_{bA} = -\frac{2F_0 R}{\pi} \qquad (103)$$

$$M_{bB} = F_0 R \left(1 - \frac{2}{\pi}\right) \tag{104}$$

Fig. 5(a) shows the displacement diagram for local and nonlocal theories. The slenderness ratio is $\lambda = 20$ and nonlocal parameter is $\gamma/R = 1$. The results of both theories are slightly different and the difference decreases when nonlocal parameter γ/R decreases. In order to investigate the effects of axial extension and shear deformation, the displacement diagram is given in Fig. 5(b). The results show that the displacements rather close to each other even if the slenderness ratio is 20. As in the local theory, it is found that the axial extension has the dominant effect.

3.3 Clamped-clamped nanobeam loaded at the midspan

The effects of several parameters on the static behavior of a circular nanobeam with clamped ends are studied in this example. The beam is loaded by a normal force F_0 at its midspan (Fig. 6).

The ratio of nonlocal and local displacements u_0/u_{0L} and moments M_{b0}/M_{b0L} at the midspan are obtained for several parameters. The effects of small scale parameter R/γ, slenderness ratio λ and opening angle θ_t on the displacement ratio u_0/u_{0L} and moment ratio M_{b0}/M_{b0L} at the midspan are studied.

Fig. 7(a) shows the displacement ratio against the small scale parameter R/γ for the beam with the opening angle of $\theta_t = 120^o$ and different slenderness ratios $\lambda = 50, 100$ and 150. The effect of small scale parameter R/γ on the displacement ratio u_0/u_{0L} is more significant for smaller slenderness values. This effect attenuates if the opening angle of the beam is decreased (i.e., the curves representing the displacement ratio becomes closer for different slenderness ratio). It is observed that, the small scale effect becomes more important for a slender beam with considerably small opening angle.

The effects of axial extension and shear deformation on the displacement are studied for several values of opening angle and slenderness ratio. For the brevity, only the results for a beam with opening angle of $\theta_t = 120^o$ and slenderness ratio of $\lambda = 50$ is given in Fig. 7(b). The difference between the results of the cases (i.e. considering axial extension or considering shear deformation) increases with the increasing slenderness. From the figure, one can see that the axial extension has the dominant effect for all opening angles and slenderness ratio. The beam theory neglecting the
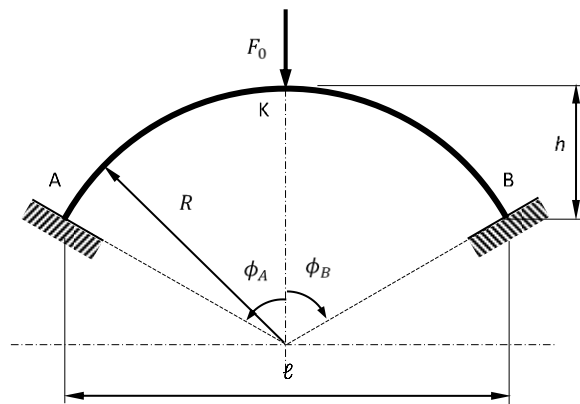

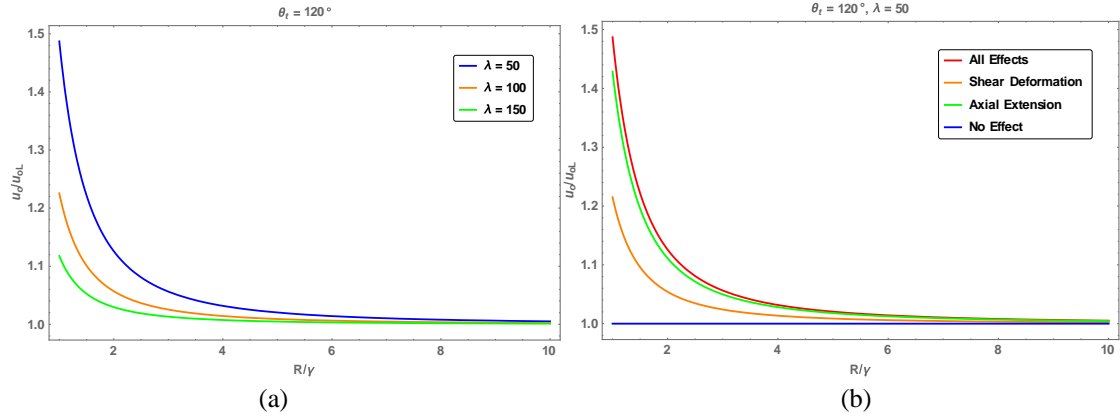Fig. 6 Clamped-clamped circular nanobeam loaded at the midspan ($\theta_t = 120^o$)

Fig. 7 The effect of R/γ on the ratio of local and nonlocal displacements u_0/u_{0L} for a clamped-clamped beam with $\theta_t = 120^o$ (a) For different values of λ (b) For different effects
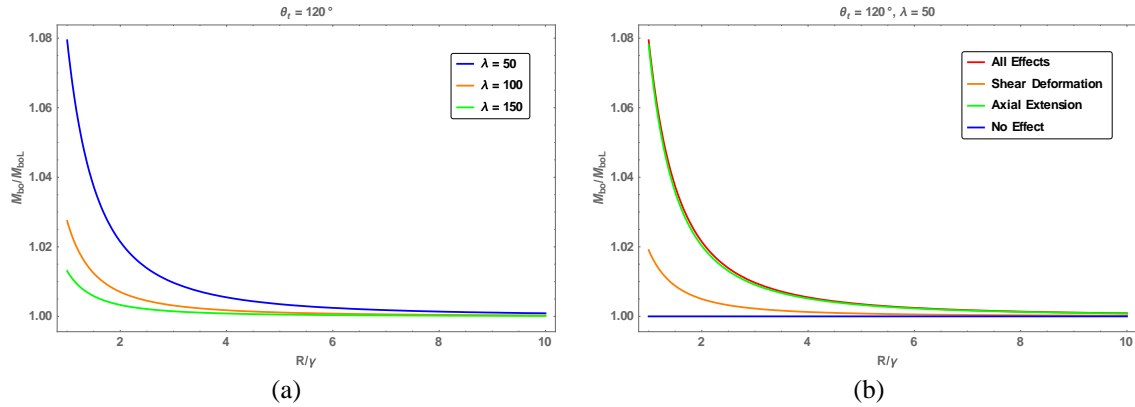

Fig. 8. The effect of R/γ on the ratio of local and nonlocal moments M_{b0}/M_{b0L} for a clamped-clamped beam with $\theta_t = 120^o$ (a) For different λ values (b) For different effects

effects of axial extension and shear deformation gives acceptable results for only a slender and deep curved beam where the bending deformation is the main effect. Moreover, when the beam is stubby, the shear deformation effect becomes also significant. The displacements for the case neglecting all effects (i.e., only the nonlocal effects of bending moment is considered) are same for both local and nonlocal theories. Similar result is obtained by Li (2015) for straight beams with concentrated loads.

Fig. 8(a) gives the diagram of the moment ratio M_{b0}/M_{b0L} against the small scale parameter R/γ for the beam with the opening angle of $\theta_t = 120^o$ and slenderness ratio of $\lambda = 50, 100$ and 150. The difference between the results of the cases (i.e., considering axial extension or considering shear deformation) increases with the increasing slenderness. This result shows that the axial extension is the main effect on the displacement ratio. Moment ratio increases with the increasing slenderness ratio for larger opening angle and the curves obtained for different slenderness ratio become closer with the decreasing opening angle.

The results of the cases considering or neglecting the axial extension and shear deformation effects for a beam with opening angle of $\theta_t = 120^o$ and slenderness ratio of $\lambda = 50$ is given in
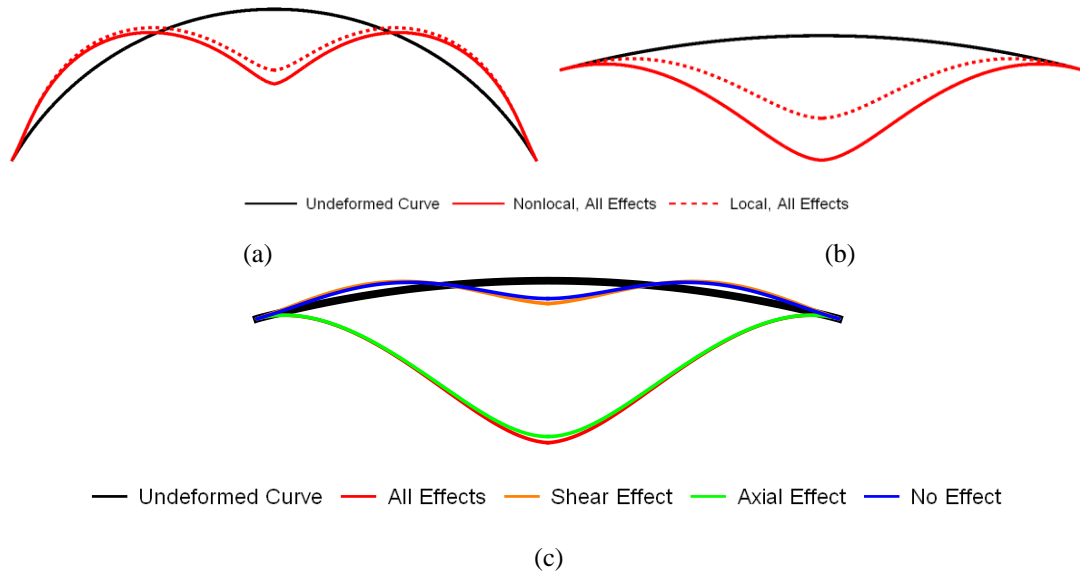
Undeformed Curve ——— Nonlocal, All Effects - - - - Local, All Effects

(a)   (b)

—— Undeformed Curve —— All Effects —— Shear Effect —— Axial Effect —— No Effect

(c)

Fig. 9 Displacements obtained by local and nonlocal theories ($R/\gamma = 1$) (a) $\theta_t = 120^o$, $\lambda = 100$; (b) $\theta_t = 30^o$, $\lambda = 100$; (c) $\theta_t = 30^o$, $\lambda = 100$

Fig. 8(b). Axial extension is the main contributing effect for all opening angle, as expected. Moment ratio increases with decreasing opening angle for all slenderness ratio.

As it is well known from the local theory, the Euler beam theory gives acceptable results for a slender and deep curved beam, but the results are not reasonable when the curved beam is shallow. Deep and shallow curved beams exhibit different static and dynamic behavior (Tufekci and Arpaci 2006, Tufekci 2001). A shallow curved beam deforms along a different path representing another characteristic deformed shape.

In order to exhibit the effect of the shallowness h/ℓ (Fig. 2), a clamped-clamped beam in Fig. 6 is considered here. The displacements obtained by local and nonlocal theories are given in Fig. 9(a) for $\theta_t = 120^o$, $\lambda = 100$ and in Fig. 9(b) for $\theta_t = 30^o$, $\lambda = 100$. The dashed lines show the results of local theory; the solid lines show the results of nonlocal theory. The deformation of nonlocal theory is significantly different than that of the local theory. The ratio of the displacements at the midspan increases with the decreasing opening angle, and it decreases with the increasing small scale parameter.

In Fig. 9(c), the displacement curves obtained by nonlocal theory with the cases considering (red line) and neglecting (blue line) the effects of axial extension and shear deformation. For $\theta_t = 30^o$ and $\lambda = 100$, not only the displacements at the crown but also the characteristics of deformed shapes are different. The effect of axial extension is significant for a shallow curved beam even if it is slender. Thus, the realistic deformed shape of a shallow beam cannot be obtained by neglecting the effects of axial extension and shear deformation. It should be noted that the shallow beam with opening angle of 30° and slenderness ratio of 100 is still slender in this example.

Fig. 10 gives the effects of small scale parameter, slenderness ratio and opening angle on the displacement ratio of a clamped-clamped beam. The effect of small scale parameter on the displacement ratio of a beam with $\theta_t = 120^o$ increases with decreasing slenderness ratio (Fig.

(a) $\theta_t = 120^o$ (b) $\lambda = 150$
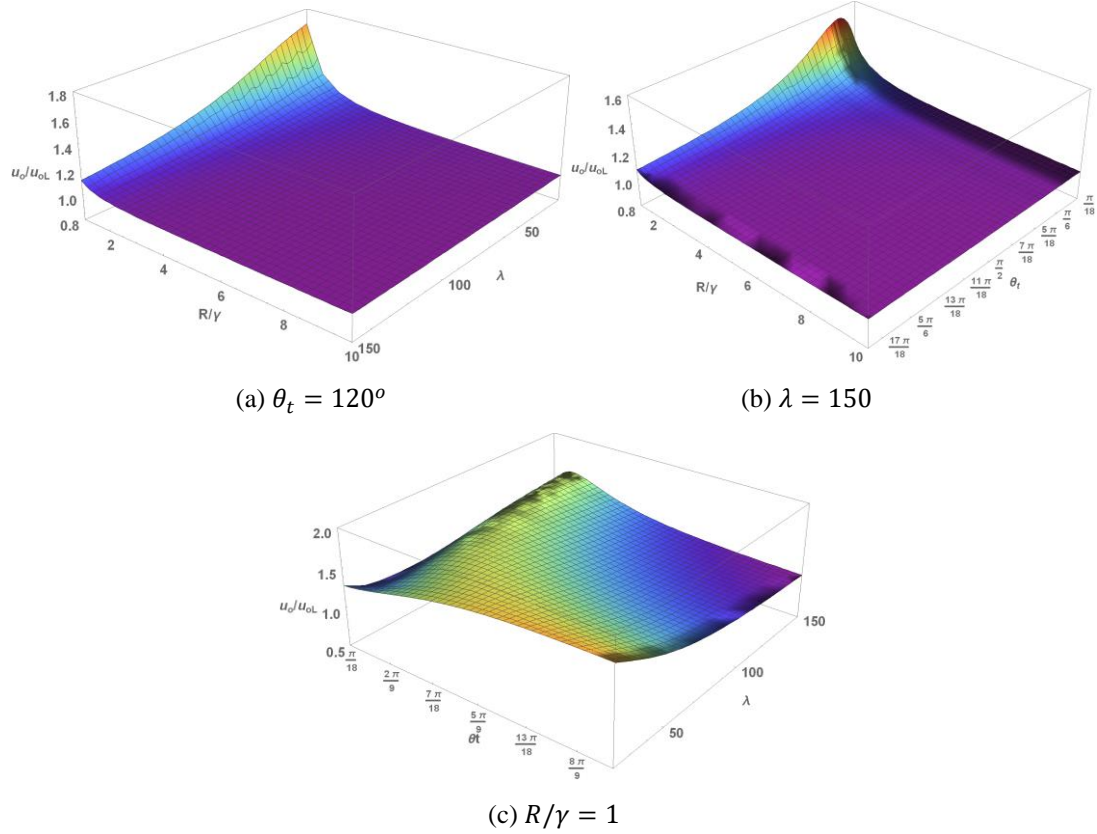
(c) $R/\gamma = 1$

Fig. 10 The effects of small scale parameter, opening angle and slenderness ratio on the displacement ratio of a clamped-clamped beam

10(a)). The displacement ratio of a beam with $\lambda = 150$ has maximum value at the opening angle around 30° for all R/γ values (Fig. 10(b)). The effect of opening angle on the displacement ratio increases, then decreases gradually for smaller slenderness ratio (Fig. 10(c)). The change is more significant for larger values of slenderness ratio.

Fig. 11 shows the change of moment ratio M_{b0}/M_{b0L} with the small scale parameter, opening angle and slenderness ratio. The small scale parameter slightly affects the moment ratio for slender beams while considerable changes are observed for beams with smaller slenderness ratio (Fig. 11(a)). The moment ratio increases for small scale parameter and/or for small opening angle. The moment ratio of a beam with $\lambda = 150$ has a maximum value at the opening angle around $\theta_t = 30^o$ for all R/γ values, and a sharp decrease is observed for smaller angle (Fig. 11(b)). When the opening angle increases, the moment ratio increases for smaller angle, and then decreases gradually afterwards. However; for larger slenderness ratio, this change is more significant. (Fig. 11(c)).

The diagrams of rotation angle (Ω_b), binormal moment (M_b), tangential force (F_t) and normal force (F_n) diagrams of the beam with $R/\gamma = 1$, $\theta_t = 120^o$ and $\lambda = 50$ are shown in Fig. 12. Solid red line represents the results of nonlocal theory and dashed red line represents those of the local theory.
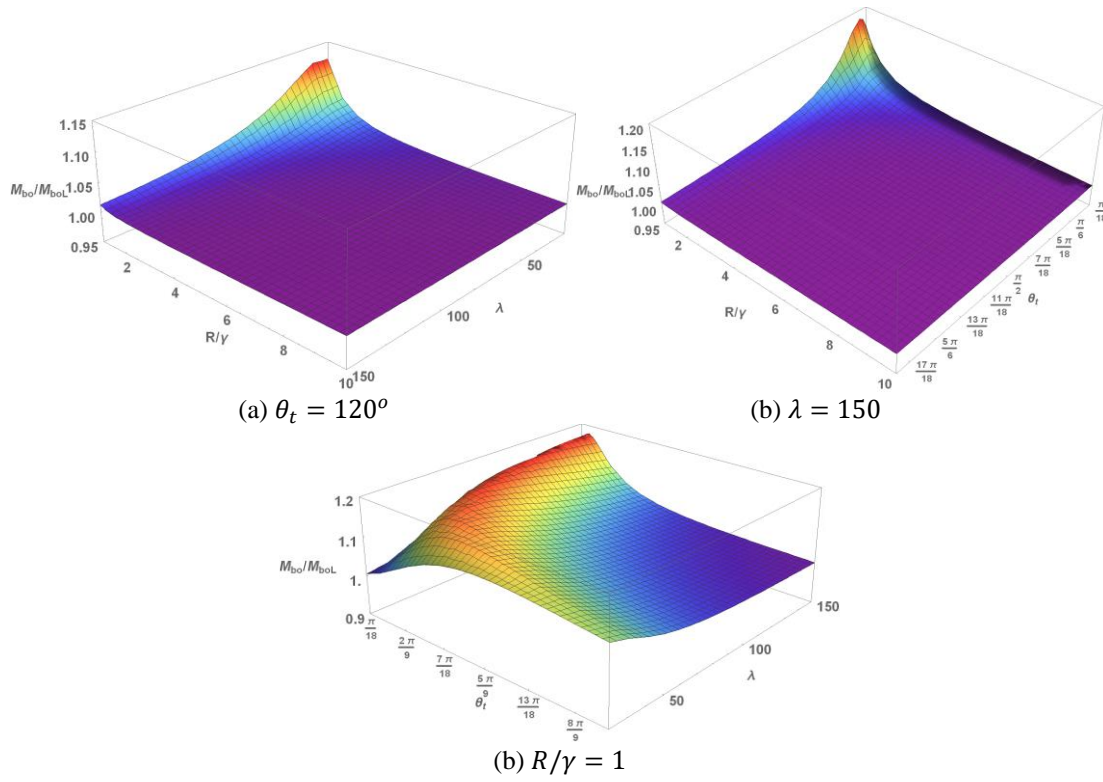
(a) $\theta_t = 120^o$

(b) $\lambda = 150$

(b) $R/\gamma = 1$

Fig. 11 The effects of small scale parameter, slenderness ratio and opening angle on the moment ratio of a clamped-clamped circular beam

(a)

(b)

(c)

(d)

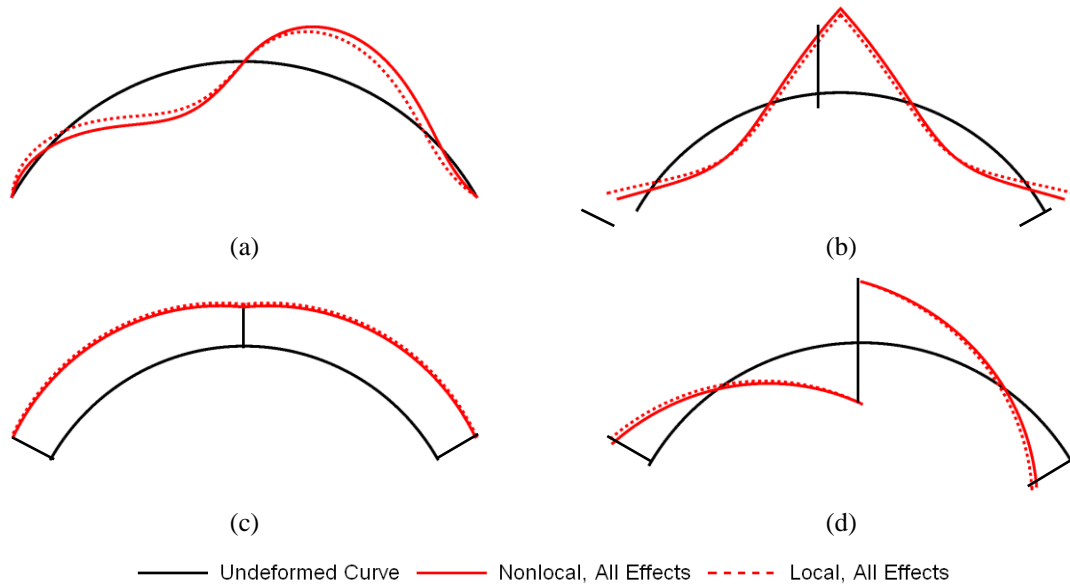—— Undeformed Curve —— Nonlocal, All Effects - - - - Local, All Effects

Fig. 12 (a) Slope (b) Binormal moment, (c) Tangential force, (d) Normal force diagrams of the beam with $R/\gamma = 1$, $\theta_t = 120^o$ and $\lambda = 50$

3.4 Effect of boundary conditions

In the previous example, a clamped-clamped beam is investigated in details. In this section, the effects of boundary conditions (i.e., hinged-clamped and hinged-hinged) on the static behavior of nanobeam are investigated in details.

The effects of small scale parameter, slenderness ratio and opening angle on the displacement and moment ratio of a hinged-clamped and hinged-hinged beams are studied. The results are not given here for brevity, since they are similar to the ones obtained for a clamped-clamped beam (see Figs. 10, 11). The diagrams of displacement, rotation angle (Ω_b), binormal moment (M_b), tangential force (F_t) and normal force (F_n) diagrams of the hinged-clamped beam with $R/\gamma = 1$, $\theta_t = 120^o$ and $\lambda = 50$ are shown in Fig. 13. The differences between the results of displacement and rotation angle obtained from local and nonlocal theories are larger than those of clamped-clamped beams.

Fig. 14 shows the change of displacement ratio u_0/u_{0L} against the small scale parameter R/γ for different boundary conditions. Here, the opening angle is $\theta_t = 120^o$ and slenderness ratio is $\lambda = 150$. The clamped-clamped beam is affected most by the small scale parameter and hinged-clamped and hinged-hinged are the following boundary conditions, respectively. If the slenderness ratio decreases for the same opening angle, the curves become closer, and the scale effect increases considerably.
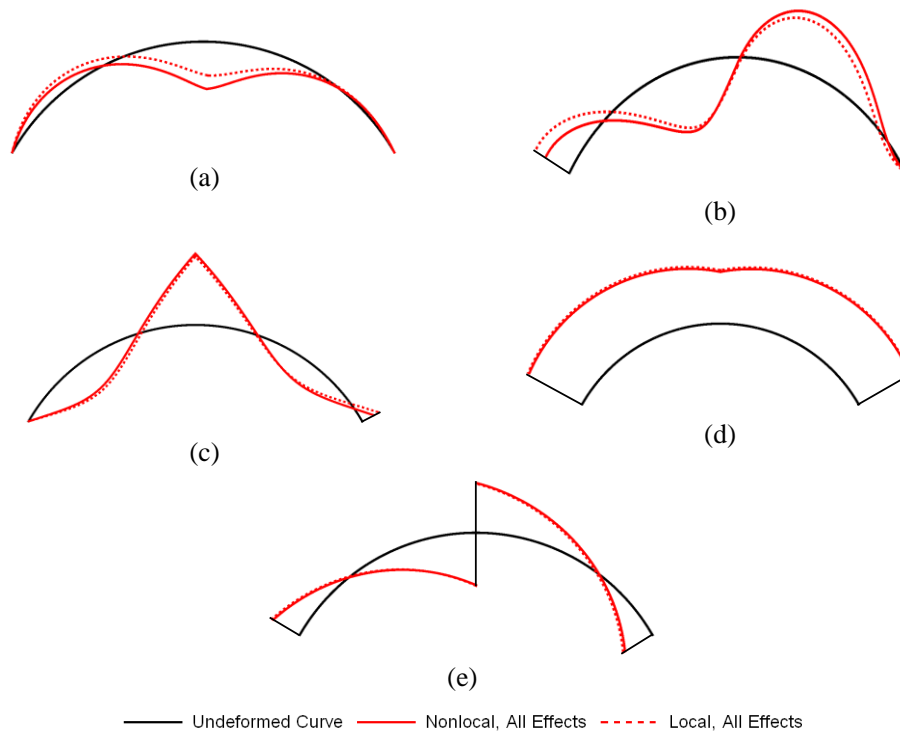

Fig. 13 The nonlocal and local (a) displacements, (b) rotation angles, (c) binormal moments, (d) tangential forces, (e) normal forces of a hinged-clamped beam ($\theta_t = 120^o$, $\lambda = 50$, $R/\gamma = 1$)

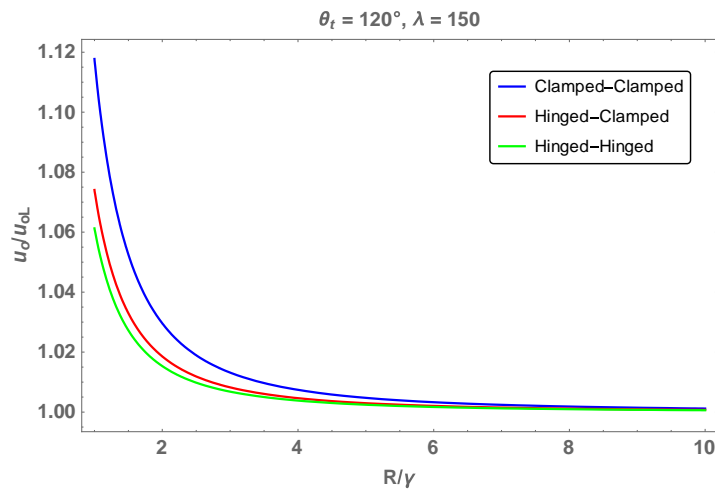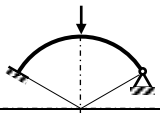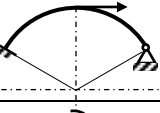Fig. 14 The effects of small scale parameter R/γ on the displacement ratio for several boundary conditions ($\theta_t = 120^o$, $\lambda = 150$)

Table 1 The displacement and rotation angle ratio of beams with various boundary and loading conditions ($\theta_t = 120^o$, $\lambda = 50$, $R/\gamma = 1$)

		All effects	Axial Ext.	Shear Def.	No Effect
	$\dfrac{u_0}{u_{0L}}$	1.36406	1.29453	1.13543	1
	$\dfrac{w_0}{w_{0L}}$	1.17921	1.14423	1.04743	1
	$\dfrac{\Omega_{b0}}{\Omega_{b0L}}$	0.96825	0.97567	0.99293	1
	$\dfrac{w_0}{w_{0L}}$	0.96825	0.97567	0.99293	1
	$\dfrac{\Omega_{b0}}{\Omega_{b0L}}$	1.01987	1.00237	1.01758	1
	$\dfrac{u_0}{u_{0L}}$	1.48699	1.42853	1.21499	1
	$\dfrac{w_0}{w_{0L}}$	1.37311	1.30450	1.13453	1
	$\dfrac{\Omega_{b0}}{\Omega_{b0L}}$	0.96583	0.93209	1.02748	1
	$\dfrac{u_0}{u_{0L}}$	2.03697	1.01461	1.02824	1
	$\dfrac{\Omega_{b0}}{\Omega_{b0L}}$	1.04750	1.00606	1.04238	1

Table 1 Continued

	$\dfrac{u_0}{u_{0L}}$	1.40005	1.33234	1.15290	1
	$\dfrac{\Omega_{b0}}{\Omega_{b0L}}$	0.66189	0.70091	0.93618	1
	$\dfrac{w_0}{w_{0L}}$	1.28485	1.22737	1.09486	1
	$\dfrac{\Omega_{b0}}{\Omega_{b0L}}$	0.979295	0.96171	1.01690	1
	$\dfrac{u_0}{u_{0L}}$	0.66189	0.70091	0.93618	1
	$\dfrac{\Omega_{b0}}{\Omega_{b0L}}$	1.04033	1.00692	1.03503	1

In Table 1, the displacement ratio u_0/u_{0L} or w_0/w_{0L} and rotation angle ratio Ω_{b0}/Ω_{b0L} are given for several loading and boundary conditions. The effects of axial extension and shear deformation is investigated. The beam has $\theta_t = 120^o$, $\lambda = 50$, $R/\gamma = 1$. The axial extension has the dominant effect for all loading and boundary conditions. The shear deformation effect must be considered for such a stubby beam in order to obtain a satisfactory result, as it is expected.

3.5 Beam with nonsymmetrical boundary and loading conditions

A circular nanobeam with non-symmetrical boundary and loading conditions, which is not available in the literature, is studied in this section. A hinged-clamped circular beam with opening angle of $\theta_t = 120°$, slenderness ratio of $\lambda = 50$ and small scale parameter of $R/\gamma = 1$ is loaded at the coordinate of $\theta_K = 30°$ with a normal force F_{nK} (Fig. 15). The displacement, rotation angle, binormal moment, normal and tangential forces are given in Fig. 16. The results are obtained by both nonlocal and local theories for the case considering all effects. As seen from the figure, the displacement and rotation angle are slightly different than those of local theory. The difference disappears for higher values of R/γ. Minor differences are observed for the force and moment diagrams.
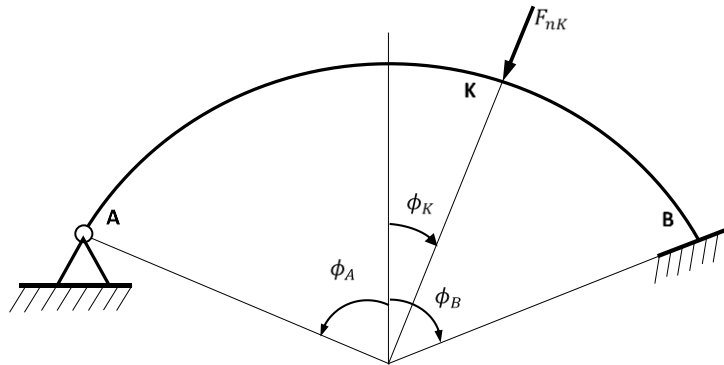
Fig. 15 A hinged-clamped circular beam with nonsymmetrical loading conditions.
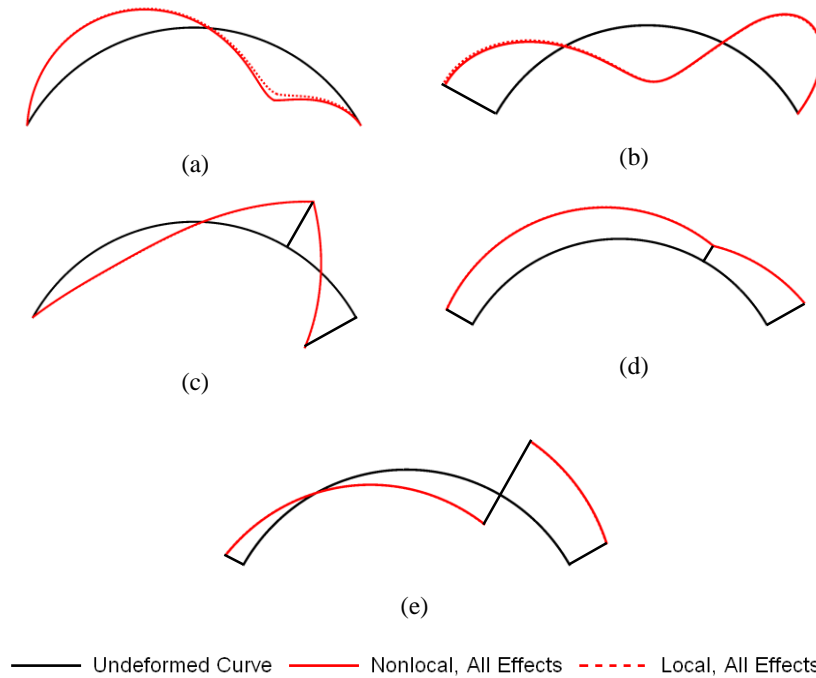
Fig. 16 (a) Displacement, (b) Rotation angle (c) Binormal moment, (d) Tangential force, (e) Normal force diagrams of hinged-clamped beam loaded with F_{nK} at $\theta_K = 30^o$ ($\theta_t = 120^o$, $\lambda = 50$, $R/\gamma = 1$)

4. Conclusions

A new size-dependent general beam theory is presented within the framework of Eringen's nonlocal elasticity theory for static behavior of curved nanobeams. Nonlocal constitutive equations are implemented in the classical beam equations. Axial extension and shear deformation effects and their size-dependent effects along with the size-dependent effects of bending moment are incorporated in the analytical model. Initial value method is used for the exact solution and the results are obtained analytically.

Other modeling techniques are suffering from some shortcomings. Atomistic approach is incapable of modeling complex atomic structures and computationally expensive. On the other hand, classical continuum approach gives relatively simple formulations but it is inadequate for modeling because of the size-free deficiency. In most of the studies, nanobeams are assumed to be perfectly straight beams, but they may also be fabricated curved to be used as sensors, resonators for nanotechnology applications. Motivated by this fact, the nonlocal beam equations are obtained and an exact solution is developed for the static problems of planar curved nanobeams. The equations provide sufficient generality in the choice of loading and boundary conditions. Main contribution of this study is to give the exact analytical solutions for the circular curved beams with uniform cross-section.

Illustrative examples of circular curved nanobeams bearing concentrated loads are discussed to highlight the effects of nonlocal parameter, axial extension, shear deformation, slenderness ratio,

opening angle, loading and boundary conditions as well as the connections between this nonlocal beam model and classical (local) beam theory.

For a slender clamped-clamped beam with opening angle $\theta_t = 120°$ loaded with a normal force at the midspan; if the small scale parameter R/γ and slenderness ratio λ decrease, the displacement ratio u_0/u_{0L} increases and similarly moment ratio M_{b0}/M_{b0L} is also increases. When the small scale parameter R/γ and opening angle θ_t decreases, the displacement ratio u_0/u_{0L} and moment ratio M_{b0}/M_{b0L} increases. For smaller opening angle, the ratio of displacements and moments decreases slightly. For smaller values of slenderness ratio, if opening angle θ_t increases the ratio of displacements and moments increase and then decreases gradually. For larger values of slenderness ratio, the change is more significant.

Other types of boundary and loading conditions are also investigated and similar results to are obtained. Besides, the effects of axial extension and shear deformation and also shallowness are studied and it is found that the results are similar to those of the local theory.

The results of displacement and rotation angle ratio are tabulated for all classical boundary conditions and loading types, considering the axial extension and shear deformation effects.

An illustrative example for unsymmetrical loading and boundary conditions is also studied and the results are given in details.

While only uniform circular nanobeams bearing concentrated loads are investigated in this paper, the equations can easily be expanded to provide sufficient generality in the choice of loading and geometry. Based on the analysis presented here, it is also possible to investigate the dynamics of curved nanobeams. Also, for engineering applications, it may be possible to develop an exact nonlocal beam finite element.

Advances in nanoscience and nanotechnology shaped the modern world in the last decade. Theory, modeling and simulation have played a critical role in these advances. With the solution method proposed herein, it would be very helpful in design and fabrication of curved beam components in MEMS and NEMS applications, particularly those whose main duties are to transfer securely the applied forces.

It is expected that the results obtained from the present study are got to instruct the engineering design of nano devices.

Acknowledgments

References

Abramowitz, M. and Stegun, I.A. (1972), *Handbook of Mathematical Functions with Formulas, Graphs, and Mathematical Tables*, 9th Printing, Dover, New York, NY, USA.

Akgoz, B. and Civalek, O. (2013), "Buckling analysis of linearly tapered micro-columns based on strain gradient elasticity", *Struct. Eng. Mech.*, **48**(2), 195-205.

Alotta, G., Failla, G. and Zingales, M. (2014), "Finite element method for a nonlocal Timoshenko beam model", *Finite Elem. Anal. Des.*, **89**, 77-92.

Arash, B., Wang, Q. and Duan, W.H. (2011), "Detection of gas atoms via vibration of graphenes", *Phys. Lett. A*, **375**(24), 2411–2415.

Behera, L. and Chakraverty, S. (2014), "Free vibration of nonhomogeneous Timoshenko nanobeams", *Meccanica*, **49**(1), 51-67.

Berrabah, H.M., Tounsi, A., Semmah, A. and Bedia, E.A.A. (2013), "Comparison of various refined nonlocal beam theories for bending, vibration and buckling analysis of nanobeams", *Struct. Eng. Mech.*, **48**(3), 351-365.

Bradshaw, R.D., Fisher, F.T. and Brinson, L.C. (2003), "Fiber waviness in nanotube-reinforced polymer composites-II: modeling via numerical approximation of the dilute strain concentration tensor", *Compos. Sci. Technol.*, **63**(11), 1705-1722.

Craighead, H.G. (2000), "Nanoelectromechanical systems", *Science*, **290**(5496), 1532-153.

Ekinci, K.L. (2005), "Electromechanical transducers at the nanoscale: Actuation and sensing of motion in nanoelectromechanical systems (NEMS)", *Small*, **1**(8-9), 786-797.

Eringen, A.C. (1983), "Linear theory of nonlocal elasticity and dispersion of plane waves", *J. Appl. Phys.*, **54**, 4703-4710.

Fisher, F.T., Bradshaw, R.D. and Brinson, L.C. (2003), "Fiber waviness in nanotube-reinforced polymer composites-I: Modulus predictions using effective nanotube properties", *Compos. Sci. Technol.*, **63**(11), 1689-1703.

Guo, R., Barisci, J.N., Innis, P.C., Too, C.O., Wallace, G.G. and Zhou, D. (2000), "Electrohydrodynamic polymerization of 2-methoxyaniline-5-sulfonic acid", *Synthetic Met.*, **114**(3), 267-272.

Hadjesfandiari, A.R. and Dargush, G.F. (2011), "Couple stress theory for solids", *Int. J. Solid. Struct.*, **48**(18), 2496-2510.

Hu, Y.G., Liew, K.M. and Wang, Q. (2009), "Nonlocal elastic beam models for flexural wave propagation in double-walled carbon nanotubes", *J. Appl. Phys.*, **106**(4):044301.

Huang, C., Ye, C., Wang, S., Stakenborg, T. and Lagae, L. (2012), "Gold nanoring as a sensitive plasmonic biosensor for on-chip DNA detection", *Appl. Phys. Lett.*, **100**, 173114.

Joshi, A.Y., Sharma, S.C. and Harsha, S.P. (2010) "Dynamic analysis of a clamped wavy single walled carbon nanotube based nanomechanical sensors", *J. Nanotechnol. Eng. Med.*, **1**, 031007-7.

Kong, J., Franklin, N.R., Zhou, C.W., Chapline, M.G., Peng, S., Cho, K. and Dai, H.J. (2000), "Nanotube molecular wires as chemical sensors", *Science*, **287**, 622-625.

Kong, X.Y., Ding, Y., Yang, R. and Wang, Z.L. (2004), "Single-crystal nanorings formed by epitaxial self-coiling of polar nanobelts", *Science*, **303**, 1348-1351.

Li, C. (2013), "Size-dependent thermal behaviors of axially traveling nanobeams based on a strain gradient theory", *Struct. Eng. Mech.*, **48**(3), 415-434.

Li, C. (2014), "A nonlocal analytical approach for torsion of cylindrical nanostructures and the existence of higher-order stress and geometric boundaries", *Compos. Struct.*, **118**, 607-621.

Li, C. and Chou, T.W. (2003), "Single-walled carbon nanotubes as ultra-high frequency nanomechanical resonators", *Phys. Rev. B*, **68**(7), 073405.

Li, C., Li, S., Yao, L.Q. and Zhu, Z.K. (2015a),"Nonlocal theoretical approaches and atomistic simulations for longitudinal free vibration of nanorods/nanotubes and verification of different nonlocal models", *Appl. Math. Model.*, **39**, 4570-4585.

Li, C., Yao, L.Q., Chen, W.Q and Li, S. (2015b), "Comments on nonlocal effects in nano-cantilever beams", *Int. J. Eng. Sci.*, **87**, 47-57.

Liu, Y.P. and Reddy, J.N. (2011), "A nonlocal curved beam model based on a modified couple stress theory", *Int. J. Struct. Stab. Dyn.*, **11**(3), 495-512.

Mayoof, F.N. and Hawwa, M.A. (2009), "Chaotic behavior of a curved carbon nanotube under harmonic excitation", *Chaos Solit. Fract.*, **42**(3), 1860-1867.

McFarland, A.W. and Colton, J.S. (2005), "Role of material microstructure in plate stiffness with relevance to microcantilever sensors", *J. Micromech. Microeng.*, **15**, 1060-1067.

Paola, M.D., Failla, G. and Zingales, M. (2013), "Non-local stiffness and damping models for shear-

deformable beams", *Eur. J. Mech. A-Solid.*, **40**, 69-83.

Peddieson, J., Buchanan, G.R. and McNitt, R.P. (2003), "Application of nonlocal continuum models to nanotechnology", *Int. J. Solid. Struct.*, **41**, 305-312.

Polizzotto, C., Fuschi, P. and Pisano, A.A. (2006), "A nonhomogeneous nonlocal elasticity model", *Eur. J. Mech. A-Solid.*, **25**(2), 308-333.

Povstenko, Y.Z. (1995), "Straight disclinations in nonlocal elasticity", *Int. J. Eng. Sci.*, **33**(4), 575-582.

Pradhan, S.C. and Sarkar, A. (2009), "Analyses of tapered fgm beams with nonlocal theory", *Struct. Eng. Mech.*, **32**(6), 811-833.

Reddy, J.N. (2007), "Nonlocal theories for bending, buckling and vibration of beams", *Int. J. Eng. Sci.*, **45**, 288-307.

Roukes, M. (2001), "Nanoelectromechanical systems face the future", *Phys. World*, **14**, 25-31

Sudak, L.J. (2003), "Column buckling of multi-walled carbon nanotubes using nonlocal elasticity", *J. Appl. Phys.*, **94**, 7281.

Taghizadeh, M., Ovesy, H.R. and Ghannadpour, S.A.M. (2015), "Nonlocal integral elasticity analysis of beam bending by using finite element method", *Struct. Eng. Mech.*, **54**(4) 755-769.

Treacy, M.M.J., Ebbesen, T.W. and Gibson, J.W. (1996), "Exceptionally high Young's modulus observed for individual carbon nanotubes", *Nature*, **381**(6584), 678-680.

Tufekci, E. (2001), "Exact solution of free in-plane vibration of shallow circular arches", *Int. J. Struct. Stab. Dyn.*, **1**, 409-428.

Tufekci, E. and Arpaci, A. (2006), "Analytical solutions of in-plane static problems for non-uniform curved beams including axial and shear deformations", *Struct. Eng. Mech.*, **22**(2), 131-150.

Wang, L.F. and Hu, H.Y. (2005), "Flexural wave propagation in single-walled carbon nanotubes", *Phys. Rev. B*, **71**(19) 195412.

Wang, Q. (2005), "Wave propagation in carbon nanotubes via nonlocal continuum mechanics", *J. Appl. Phys.*, **89**, 124301.

Wang, Q. and Shindo, Y. (2006), "Nonlocal continuum models for carbon nanotubes subjected to static loading", *J. Mech. Mater. Struct.*, **1**(4), 663-680.

Zemri, A., Houari, M.S.A., Bousahla, A.A. and Tounsi, A. (2015), "A mechanical response of functionally graded nanoscale beam: an assessment of a refined nonlocal shear deformation theory beam theory", *Struct. Eng. Mech.*, **54**(4), 693-710.

Zhang, Z., Wang C.M. and Challamel, N. (2015), "Eringen's length-scale coefficients for vibration and buckling of nonlocal rectangular plates with simply supported edges", *J. Eng. Mech.*, **141**(2), 04014117.

Zhao, Q., Gan, Z.H. and Zhuang, O.K. (2002), "Electrochemical sensors based on carbon nanotubes", *Electroanal.*, **14**(23), 1609-13.

CC